A Spectroscopic Analysis of Poly(lactic acid) Structure

Shuhui Kang and Shaw Ling Hsu*

Polymer Science and Engineering Department and Materials Research Science and Engineering Center, University of Massachusetts, Amherst, Massachusetts 01003

Howard D. Stidham

Chemistry Department, University of Massachusetts, Amherst, Massachusetts 01003

Patrick B. Smith and M. Anne Leugers

Analytical Sciences, The Dow Chemical Company, Midland, Michigan 48667

Xiaozhen Yang

Polymer Physics Laboratory, The Center for Molecular Science, Institute of Chemistry, Chinese Academy of Sciences, Beijing 100080, China

Received September 14, 2000; Revised Manuscript Received March 5, 2001

ABSTRACT: A vibrational analysis has been carried out to analyze the chain conformation of poly(lactic acid) in the crystalline state. In conjunction with a normal-coordinate analysis, the Raman spectrum has yielded data regarding conformational distributions. Raman spectra of different helices were simulated using previously published structures, force constants, and intensity parameters. Some of the chain conformations predicted are inconsistent with the data. Only one of the four 3_1 helical structures predicted by conformational analysis agrees well with experiment. This analysis provides a new understanding regarding the relative probability of a 10_3 or 3_1 helix for poly(lactic acid).

Introduction

Poly(lactic acid), as a biodegradable polymer, has tremendous potential in both traditional and nontraditional applications where thermoplastics are employed. Since it degrades to nontoxic lactic acid, which is naturally present in the human body, poly(lactic acid) can be used in bone fracture fixation,[1] in drug delivery systems,[2,3] in prosthetic devices,[4] as surgical suture, or in blood vessel repair.[5] Furthermore, the attribute of biodegradability makes it a promising material for many disposable products, such as baby diapers, plastic bags, and films. Poly(lactic acid) is also melt-spinnable and has very good fiber- and film-forming properties. Recently, applications involving high-strength fibers and films were reported.[6]

Poly(lactic acid) as a commodity polymer exhibits several drawbacks, which limit its utility in some applications. Depending on chain configuration, poly(lactic acid) can crystallize extremely quickly, degrading mechanical properties.[7,8] Highly crystalline poly(lactic acid) cannot be resorbed completely after long-term hydrolysis, and the remaining crystalline debris can induce secondary tissue reactions.[9] This has been overcome to some extent by copolymerizing with other functional groups or with its enatiomer to increase the degradation rate and to decrease the crystallization kinetics.[4] An alternative method is to blend or alloy poly(lactic acid) with other polymers.

Many aspects of poly(lactic acid) present exciting areas of research. The crystallization behavior of this polymer either pure, as a copolymer, or in blends remain poorly defined. Even the crystalline structure of the homopolymer has yet to be assigned definitively. An early X-ray experiment on fiber samples showed that a 10_3 helix exists in a crystalline phase.[10] Subsequently, it was pointed out those two crystalline structures, α and β, existed in solution-spun poly(lactic acid).[6] The exact form obtained depended on the spinning and drawing conditions employed. A low drawing temperature and/or low hot-draw ratios will produce the pseudo-orthorhombic α structure, which has a 10_3 helix. At higher drawing temperatures and/or higher draw ratios, an orthorhombic β structure is produced which has a 3_1 helix. Molecular simulation used to study the relationship between packing and conformation suggested that neither a regular 3_1 nor a regular 10_3 helix can fit the experimental data well.[11] The crystalline structure thus appears to be a distorted 3_1 helix, which is a modification of a regular 3_1 helix. There appears to be no definitive determination of the crystalline structure for a bulk sample.

To predict and explain the crystal structure of poly(lactic acid), a rotational isomeric state (RIS) model for poly(L-lactic acid) and an associated conformational energy map was developed.[12] There are four minimum-energy states corresponding to four distinct conformations. Because of electron delocalization, the structure of the C−O (ester) bond was assumed to maintain the trans conformation.[10] The other two bonds, O−C and C−C, are flexible and can assume the following conformations: tt (−160°, 160°), tg (−160°, −48°), gt (−73°, 160°), and gg (−73°, −48°). The gt conformation has the lowest energy and corresponds to either a 3_1 or a 10_3 helix.[12] The second lowest energy minimum, gg, is predicted to be only 0.08 kcal/mol higher in energy and should account for 37% of chain conformers at 25 °C. The characteristic ratio was then calculated to be about 2.0 based on this model.[12] This prediction is further supported by a light scattering experiment carried out

* To whom correspondence should be addressed.

10.1021/ma0016026 CCC: $20.00
Published on Web 05/19/2001

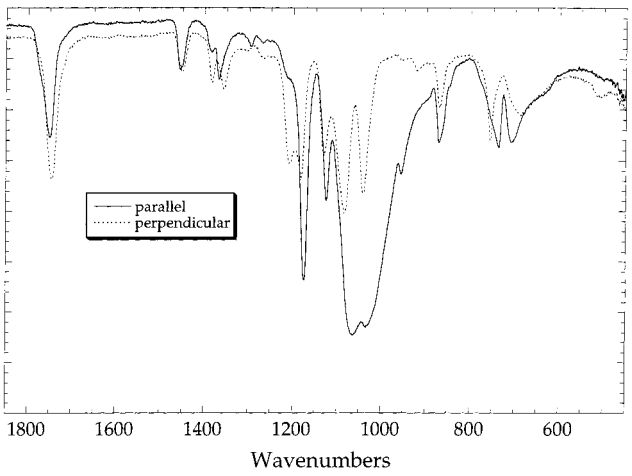

Figure 1. Polarized infrared spectra of drawn poly(lactic acid) film taken by the ATR technique.

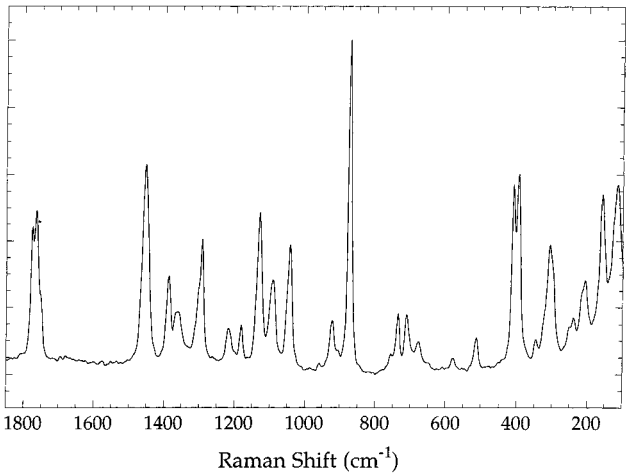

Figure 2. Raman spectra of highly crystalline poly(lactic acid) sample.

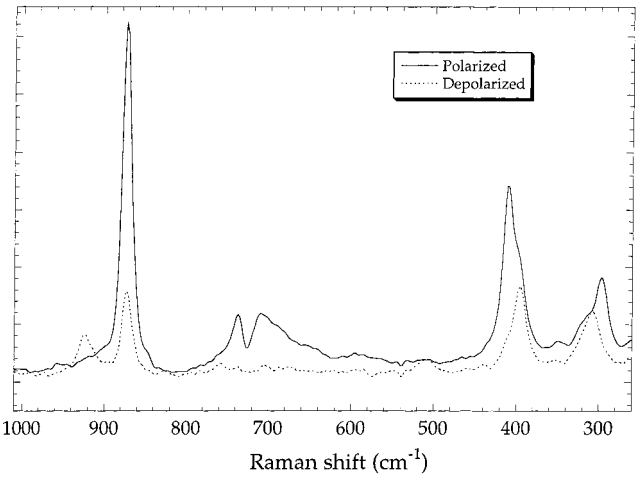

Figure 3. Polarized Raman spectra of poly(lactic acid). The drawing direction of the sample is put parallel to laser polarization direction. Polarized spectra are obtained by collecting scattered light along the direction of sample drawing; depolarized spectra are collected perpendicular to drawing direction.

by the same group.[13] Subsequent experimental data suggest the characteristic ratio can be much higher than originally postulated.[14] In addition, the fact that the mechanical properties measured for poly(lactic acid) suggests that a low value of characteristic ratio may not be justified. These new experimental data and analyses raise some doubt regarding the rotational isomeric state model from which the low characteristic ratio was deduced.[14]

On the basis of X-ray diffraction analysis of fiber samples, Okihara and co-workers reported that a 3_1 helix structure exists in the stereocomplex of poly(L-lactic acid) and poly(D-lactic acid). These authors fit the fiber period data with given poly(lactic acid) molecular structure parameters, and it appeared that four types of 3_1 helix may exist. A definitive conclusion was not proposed, however. In the work reported here, a vibrational spectroscopic study (Raman and infrared) was conducted in conjunction with theoretical normal-coordinate analysis to reexamine the structure of poly(lactic acid). Published structural parameters, force field parameters, and intensity parameters were used to simulate vibrational spectra of poly(lactic acid). The simulated spectra were then compared to the experimental Raman and infrared data obtained in this work. The simulations showed that distinct and definitive spectroscopic features are associated with each proposed structure and that only one of these models experiment adequately.

Experimental Section

Poly(lactic acid) pellets with less than 1% D impurity were purchased from Aldrich. Its molecular weight was approximately 85 000−100 000. Highly crystalline samples were obtained by dissolving the polymer at 130 °C in *p*-xylene and growing crystals in 0.05% solution at 80 °C. After filtration, the translucent layered single-crystal mat was annealed at 130 °C for 24 h. No degradation of polymer was observed after annealing. The crystals were dried for 3 days in a vacuum oven at room temperature.

Cargill-Dow provided a transparent and isotropic film sample with 1.4% D impurity. A DSC scan showed the degree of crystallinity was very low for the film as received. A uniaxially drawn sample was obtained by stretching the original film at 80 °C with a draw ratio equal to 5 and a strain rate of 10 cm/min. The deformed sample was still transparent with no visible voids or cracks.

Reflectance infrared spectra were obtained using a Perkin-Elmer system 2000 Fourier transform infrared spectrometer with a KRS-5 ATR attachment. Polarized spectra of 2 cm^{-1} resolution were obtained by putting the sample parallel or perpendicular to incident beam polarization. Since the incident beam does enter the sample at an angle, intensity analysis of parallel-polarized infrared spectrum may be nontrivial.[15] We have minimized the possible problem by rotating the sample with respect to the incident beam. As demonstrated below, the infrared data obtained are only used to aid the assignment of the polarized Raman-active vibrations. Raman spectra were obtained using a Bruker Fourier transform Raman spectrometer (model FRA 106). The 1.064 μm line of a Nd:YAG laser was used for excitation. The power at the sample was maintained at 200 mW. The resolution was maintained at 4 cm^{-1}, and 256 scans are signal averaged. Backscattering geometry was used. Polarized Raman spectra are obtained by installing a polarization analyzer followed by a scrambler in the path of the scattered beam. The stretching direction of the sample was placed parallel to the polarization direction of the incident beam. The polarized component was obtained by setting the analyzer parallel to the sample stretching direction while the depolarized component was obtained by setting the analyzer polarization perpendicular to the stretching direction. Polarized ATR infrared spectra are shown in Figure 1. The Raman spectrum of a highly crystalline sample is shown in Figure 2. Polarized Raman spectra for a deformed sample are shown in Figure 3.

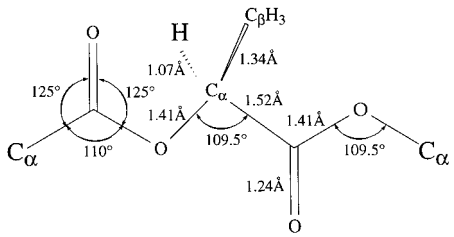

Figure 4. Chemical structure of poly(lactic acid).

Normal-Coordinate Analysis. The normal-coordinate computer program used was based on the set of programs first developed at University of Michigan.[16] Those programs have now been modified and adapted for use either with infinite chains which have well-defined chain conformations or with chains of finite length. The modifications allow calculation of the relative intensity of selected skeletal vibrations. It has recently been shown that only a very few parameters are needed to calculate the isotropic Raman scattering intensities below ~1000 cm^{-1}.[17–19] Additivity in bond polarizability derivatives is assumed. The isotropic scattering activity for mode k can be represented as

$$S_k(\text{iso}) \sim (\sum_i d_i L_{ik})^2 \tag{1}$$

where L_{ik} is the internal coordinate displacement amplitude of component i for eigenvector L_k, and d_i represents the mean polarizability derivative for internal coordinate i. The summation in eq 1 is a representation of the polarizability derivative, described in terms of the internal coordinates. The most important derivatives for *n*-alkanes or polypropylenes are associated with C−C stretch and C−C−C angle bending internal coordinates.[20–24] When the same method is applied to poly(lactic acid), the isotropic scattering activity becomes

$$S_k(\text{iso}) \sim (D_R\sum_i L^{\text{R}}_{ik} + D_S\sum_j L^{S}_{jk} + D_\omega\sum_m L^{\omega}_{mk} + D_\zeta\sum_n L^{\zeta}_{nk})^2 \tag{2}$$

where the elements of the eigenvector matrix, L^{R}_{ik} and L^{ω}_{mk}, represent the backbone C−C, C−O stretch and C−C−O, C−O−C angle bending components, and L^{S}_{jk} and L^{ζ}_{nk} represent the C═O, C−C stretch of the side chain group and C−C−C, C−C−O angle bending components containing the CH_3 groups for the normal mode k. The intensity parameters used in our calculations are 1.0 for all stretching coordinates, C−C, C═O, C−O; 0.4 for C−C−C bending; and 0.2 for all other bending. These coefficients are so chosen as they fit the experimental Raman data well.[22] They are comparable to the ones found for isotactic polypropylene,[21] syndiotactic polypropylene,[25] and poly(ethylene oxide).[22]

To transfer the force field already used successfully for other polymers, the same structure parameters were taken from the above polymers. The molecular structure parameters used in the analysis are shown in Figure 4. These were transferred from previous studies.[12,26,27] The main difference between the structure used in this work and that employed previously is that a planar structure was used for the ester group. The C−O bond length was taken to be 1.41 Å. It should be noted that this bond may be as short as 1.34 Å as listed in a previous study.[26] Figure 5 shows the definition of internal coordinates. The local symmetry coordinates used are shown in Table 1.

One requirement for accurate normal-coordinate analysis is the availability of a reliable force field. In general, only intramolecular potential energies are needed. Because poly(lactic acid) has functional groups, which have been analyzed previously, the force field used was a combination of the ones refined for polyolefins, polyethers, and polyesters.[27–29] The force constants were originally derived from smaller molecules and have been successfully used to calculate vibrational spectra of aliphatic polyethers and aromatic polyesters. Based on previous experience,[30] the force constants applicable to

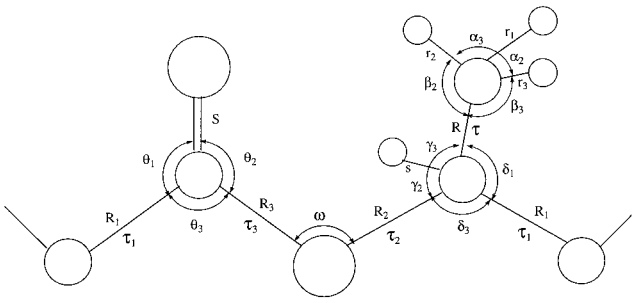

Figure 5. Internal coordinates definition for poly(L-lactic acid) molecule used in normal-coordinate analysis.

Table 1. Definition of Local Symmetry Coordinates for Poly(lactic acid)

i	group coordinates	description	designation
1	$r_1 + r_2 + r_3$	CH_3 symmetric C−H stretching	r^+
2	$2r_1 - r_2 - r_3$	CH_3 asymmetric C−H stretching	r^-
3	$r_2 - r_3$	CH_3 asymmetric C−H stretching	r^-
4	s	CH C−H stretching	s
5	R	C−CH_3 stretching	R
6	R_1	C−COO stretching	R_1
7	R_2	O−CH stretching	R_2
8	R_3	O−CO stretching	R_3
9	S	C═O stretching	S
10	$\alpha_1 + \alpha_2 + \alpha_3 - \beta_1 - \beta_2 - \beta_3$	CH_3 symmetric bending	U
11	$2\alpha_1 - \alpha_2 - \alpha_3$	CH_3 asym bending	α
12	$\alpha_2 - \alpha_3$	CH_3 asym bending	α
13	$2\beta_1 - \beta_2 - \beta_3$	CH_3 rocking	β
14	$\beta_2 - \beta_3$	CH_3 rocking	β
15	$\alpha_1 + \alpha_2 + \alpha_3 + \beta_1 + \beta_2 + \beta_3$	redundancy	$\delta\delta\delta$
16	γ_1	CH bending	γ_1
17	γ_2	CH bending	γ_2
18	γ_3	CH bending	γ_3
19	δ_1	CH_3 side chain bending	δ_1
20	δ_2	CH_3 side chain bending	δ_2
21	δ_3	skeletal CCO bending (under CH_3)	δ_3
22	$\theta_1 - \theta_2$	C═O in-plane bending	θ
23	$2\theta_3 - \theta_1 - \theta_2$	C═O deform (skeletal CCO bending)	Ω
24	$\theta_1 + \theta_2 + \theta_3$	redundancy	$\delta\delta\delta$
25	π	C═O out-of-plane bending	π
26	ω	skeletal COC bending	ω
27	τ_1	torsion C−COO	τ_1
28	τ_2	torsion O−CH	τ_2
29	τ_3	torsion O−CO	τ_3
30	τ	torsion C−CH_3	τ

individual functional groups are not a problem. Indeed, we felt that there might be a problem with the skeletal vibrations involving junctions of various functional groups. The combination of force fields from different sources, in fact, proved to be extremely satisfactory. However, some force constants cannot be directly transferred from literature, and a refinement has to be carried out. Because of differences in the definition of internal coordinates, the force constant definition may be different. The in-plane bending coordinate is an example. In this case, some force constants in previous studies are defined for the three angles, some defined for two of the three in-plane valence angles (see Table 1, nos. 22 and 23). These differences needed to be and have been reconciled in our definition of internal coordinates and local symmetry coordinates. The force constants used in this work are listed in Table 2.

Results and Discussion

The crystalline structure for poly(L-lactic acid) remains undefined. Some authors suggested it is a 10_3

Table 2. Valence Force Constants Used for Poly(lactic acid)[f]

name of group	value	name of group	value
stretch			
$C_\beta-H$	4.699[a]	$O-C_\alpha$	5.090[a]
$C_\alpha-H$	4.688[a]	C−O	6.715[b]
$C_\alpha-C_\beta$	4.261[a]	C=O	11.474[b]
$C_\alpha-C$	4.330[d]		
bend			
$H-C_\beta-H$	0.540[a]	$C-C_\alpha-O$	1.670[c]
$C_\alpha-C_\beta-H$	0.645[a]	$C_\beta-C_\alpha-C$	0.771[d]
$C_\beta-C_\alpha-H$	0.800[d]	def C=O[e]	1.967[b]
$C-C_\alpha-H$	0.618[d]	ipb C=O[e]	1.348[b]
$O-C_\alpha-H$	0.720[d]	opb C=O[e]	0.630[d]
$C_\beta-C_\alpha-O$	1.100[d]	$C-O-C_\alpha$	1.796[c]
torsion			
$\tau(C-O)$	0.017[a]	$\tau(C_\alpha-C)$	0.048[a]
$\tau(O-C_\alpha)$	0.026[a]	$\tau(C_\alpha-C_\beta)$	0.072[a]
sretch−stretch			
$C_\beta-H$, $C_\beta-H$	0.043[a]	C−O, $C_\alpha-O$	0.458[c]
$C_\alpha-C_\beta$, $C_\alpha-C$	0.154[d]	C−O, $C_\alpha-C$	0.845[d]
$C_\alpha-C_\beta$, $C_\alpha-O$	0.154[d]	$C_\alpha-C$, C=O	1.220[d]
$C_\alpha-C$, $C_\alpha-O$	0.154[d]	C−O, C=O	0.809[d]
stretch−bend			
$C_\alpha-C_\beta$, $C_\alpha-C_\beta-H$	0.328[a]	$C_\alpha-O$, $C_\beta-C_\alpha-O$	0.618[a]
$C_\alpha-C_\beta$, $C_\beta-C_\alpha-H$	0.328[a]	C_α-O, $C-C_\alpha-O$	0.618[a]
$C-C_\alpha$, $C-C_\alpha-H$	0.328[a]	$C_\alpha-O$, $C_\alpha-O-C$	0.683[d]
$O-C_\alpha$, $O-C_\alpha-H$	0.387[a]	C−O, $C-O-C_\alpha$	0.683[d]
$C_\alpha-C_\beta$, $C_\beta-C_\alpha-C$	0.417[a]	C−O, ipb C=O	0.048[d]
$C_\alpha-C_\beta$, $C_\beta-C_\alpha-O$	0.403[a]	C−O, def C=O	1.198[d]
$C_\alpha-C$, $C_\beta-C_\alpha-C$	0.417[a]	$C_\alpha-C$, def C=O	0.693[d]
C_α-C, $C-C_\alpha-O$	0.403[a]	$C_\alpha-C$, ipb C=O	0.464[c]
bend−bend			
$C_\alpha-C_\beta-H$, $C_\alpha-C_\beta-H$	−0.012[a]	$C_\beta-C_\alpha-O$, $C-C_\alpha-O$	−0.041[a]
$C_\beta-C_\alpha-H$, $C-C_\alpha-H$	0.115[d]	$C_\beta-C_\alpha-C$, $C-C_\alpha-O$	−0.041[a]
$C_\beta-C_\alpha-H$, $O-C_\alpha-H$	0.115[d]	trans $H-C_\alpha-C_\beta-H$	0.100[d]
$C-C_\alpha-H$, $O-C_\alpha-H$	0.115[d]	gauche $H-C_\alpha-C_\beta-H$	0.060[d]

[a] Directly transferred from ref 28. [b] From ref 27. [c] From ref 29. [d] Refined. [e] Constants defined in group coordinates. [f] Stretching constants are in mdyn Å^{-1}, and bending constants are in mdyn Å rad^{-2}.

helix; others prefer a similar 3_1 helix or a structure with features of the two.[6,10,11,14] Since 3_1 and 10_3 helices are so similar in structure, for simplicity, our initial analysis used a 3_1 helix. In this case, there are 9 atoms for each chemical repeat unit. Three such units with a phase angle difference of 120° form a translational repeat unit. The optical activity of such a poly(lactic acid) has 25 A modes and 26 degenerate E modes. The calculated frequencies of this model and a comparison with experimental values are listed in Table 3. The potential energy distribution of each vibration is listed in the last column.

The observed Raman and infrared vibrations shown in Figures 1 and 3 can be assigned on the basis of their frequencies and polarization characteristics. For a uniaxially oriented poly(lactic acid) sample, the A modes of a 3_1 helix are infrared-active and have transition moments parallel to the chain axis. In contrast, vibrations with transition moments perpendicular to the chain axis are E modes.[31] The analysis of optical activity associated with a helix also revealed that A modes are polarized in Raman spectra; E modes are depolarized.[32,33] In many cases, especially when features overlap, the exact assignment can only be accomplished when both the infrared and Raman data are taken into account. The simulated isotropic Raman spectrum for a 3_1 helix together with the experimental data are shown in Figure 6. The A modes are marked with an asterisk in the experimental spectrum. Virtually all the experimental data are reproduced accurately by the

Table 3. Band Assignments of 3_1 Helix Poly(lactic acid)

obsd	IR	Raman	calcd	potential energy distribution (%)
			A Mode	
1750	s	s	1750	S(87), Ω(14), R_3(11)
1455	m	s	1460, 1457	α(90), β(8)
1385	w	w	1383	U(82), γ_3(10), R(7)
1368	m	w	1363	R_3(49), θ(20), R_2(15), R_1(8)
1295	w	m	1288	γ_3(35), R_2(23), γ_2(20), U(13)
1175	s	w	1196	R_1(30), R_2(24), γ_3(24), γ_1(16)
1124	s	s	1140	γ_2(58), γ_1(32), R_2(5)
1084	vs	m	1088	R(54), β(18), δ_2(8)
1042	vs	s	1030	β(45), γ_1(27), R_1(7)
956	s	w	961	β(66), R_1(11), R_2(9), R_1(8)
873	m	vs	869	R_1(25), β(21), ω(20), R_3(18), Ω(18)
737	m	m	739	π(28), R(23), δ_3(19), θ(7)
710	m	m	706	π(41), θ(18), δ_1(12), R_3(8)
412	m	s	417	δ_2(35), R_3(13), θ(10)
350		w	355	δ_3(30), θ(27), γ_1(7)
297		m	298	δ_1(34), δ_2(29), ω(20)
250		w	250	Ω(45), R_2(32)
200		w	204	τ(86)
156		m	149	ω(35), δ_1(19), δ_3(13), Ω(10)
			E Mode	
1745	s	s	1750	S(87), Ω(13), R_3(12)
1450		s	1457	α(90), β(8)
1383	w	w	1383	U(82), γ_3(10), R(7)
1356	m	w	1350	R_3(52), θ(28), R_2(13), R_1(10)
1306	w	m	1270	γ_3(50), R_2(24), U(13)
1210	s	w	1168	R_1(32), R_2(24), β(19), γ_1(16)
1132	s	s	1125	γ_2(37), γ_1(14), R_2(20)
1084	vs	m	1096	R(40), β(19), δ_3(9)
1042	vs	s	1027	β(53), γ_1(27), R_1(7)
923	s	w	935	β(53), R_2(24), R_1(8)
873	m	vs	832	R_1(32), R(17), ω(12), R_3(13), Ω(11)
756	m	m	765	θ(18), R(11), δ_3(14), π(5)
685	m	m	709	π(61), R(9)
523	m	s	600	Ω(34), R_2(16), R_1(10)
398		w	402	θ(32), δ_3(12), δ_2(11)
315		m	338	δ_3(31), δ_2(12), Ω(20)
240		w	226	δ_1(52), δ_2(14)
200		w	204	τ(90)
156		m	156	ω(42), δ_2(22), Ω(22)

normal-coordinate analysis. This agreement in both band position and intensity suggests that the transferred structural parameters, force field, and intensity parameters are sufficiently accurate for structural analysis.

We were curious whether our spectroscopic analysis can be used to differentiate the various helices predicted. For the first structural analysis, the chain conformation corresponding to the four minima in the energy contour map has C−C, C−O bonds being tt, tg, gt, and gg. These correspond to a 2_1, 5_1, 3_1, and 4_1 helix, respectively (see Table 4). The relative energies of the minima suggest that the 3_1 helix is the most favorable one and the 4_1 helix is the second most favorable one. One would then conclude that it would be highly probable to find both 3_1 and 4_1 helices. It should be emphasized that this is a single chain calculation; intermolecular interactions have not been taken into account. According to the contour map presented in earlier work, a completely random structure would contain 55% gt conformation and 37% gg conformation. It can be assumed that the Raman band feature of such a chain would include 55% 3_1 helix (pure gt conformation) band feature and 37% 4_1 helix (pure gg conformation) band feature, respectively. By simulating the

Table 4. Helices Generated Corresponding to Energy Minima in Previously Calculated RIS Model

conformation	torsion angles (deg) (O−C_α, C_α−C)	energy minima (kcal/mol)	weight at 25 °C (%)	closest helices	torsion pairs used in helix approximation
tt	−160, 160	1.40	4.2	2_1	−180.0, 180.0
tg	−160, −48	1.52	4.0	5_1	−144.4, −53.0
gt	−73, 160	0.0	55	3_1	−80.8, 156.7
gg	−73, −48	0.08	37	4_1	−73.6, −46.2

Table 5. Torsinal Angles (deg) Used To Simulate 3_1Helix and 10_3 Poly(lactic acid) Helices

	3_1 helix	10_3 helix
torsion angles of (O−C_α, C_α−C)	−80.8, 156.7	−76.3, 168.8

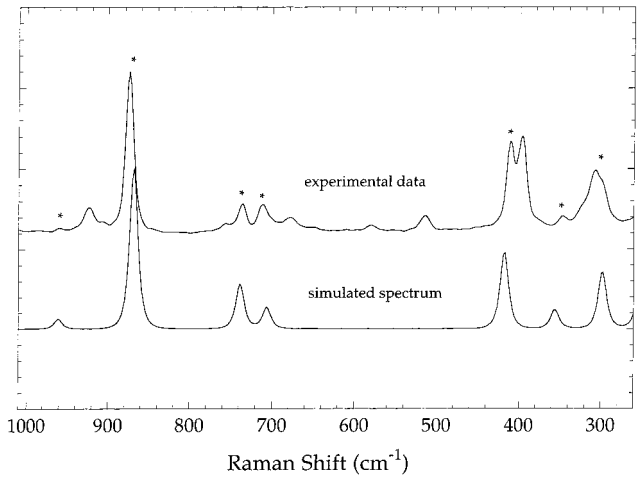

Figure 6. Measured and simulated (A modes only) Raman spectra for 3_1 helix model.

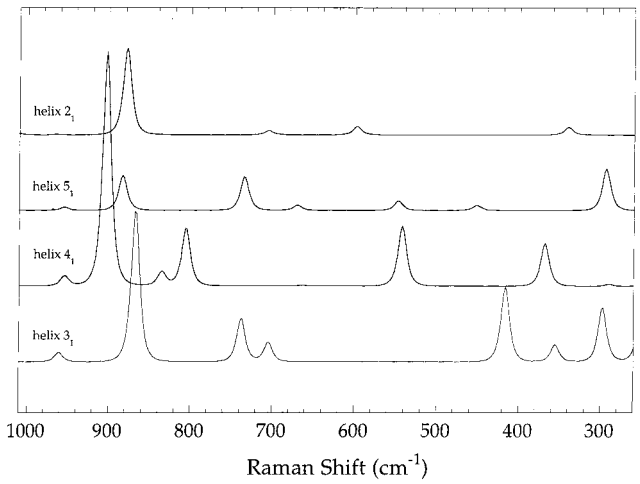

Figure 7. Calculated spectra of four helices (2_1, 3_1, 4_1, and 5_1) predicted in Brant's RIS model.

spectra for each of these helical structures, it is then possible to compare specific features of each in order to determine whether they exist in actual poly(lactic acid) crystals.

On the basis of our previous study,[34] it is known that bands in the 920, 720, 520, 412, and 398 cm^{-1} regions are most sensitive to changes in structural order. Figure 7 is the simulated spectra of the four helical structures. For a 4_1 helix, the 870 cm^{-1} band is shifted to 900 cm^{-1} and a strong band appears around 550 cm^{-1}. For 2_1 and 5_1 helices, bands also have been calculated to exist between 500 and 600 cm^{-1}, but the 400 cm^{-1} band should be absent. The features expected for the 2_1 and 5_1 helices are quite different from the actual infrared and Raman observations. Since tt and tg conformations

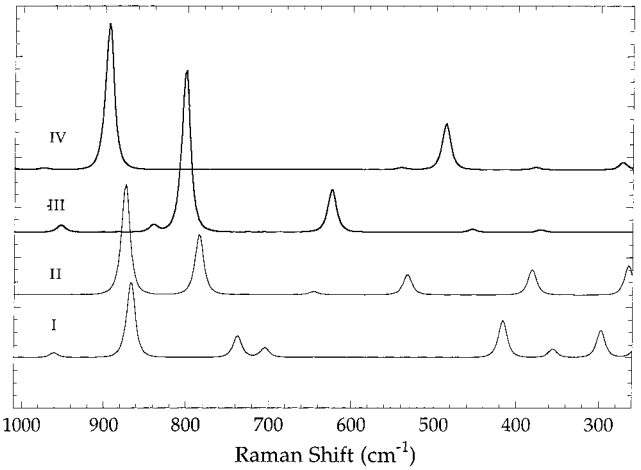

Figure 8. Calculated spectra of four 3_1 helices predicted by Okihara.[26]

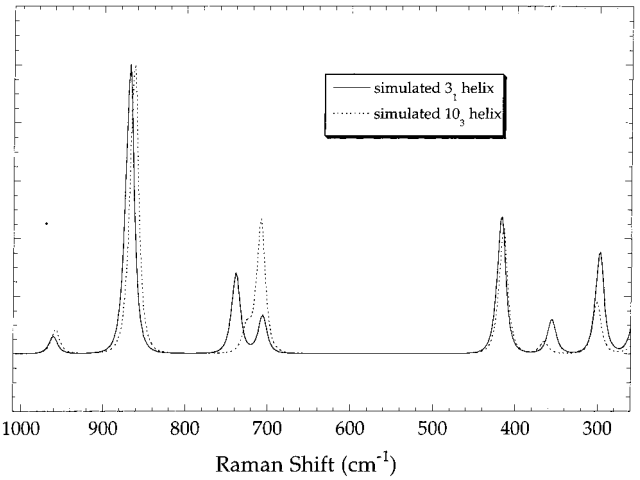

Figure 9. Calculated spectra of 3_1 and 10_3 helix structure.

have very high energy according to this model, one should expect very low probability of having a 2_1 or 5_1 helix. However, as the gg conformation has very low energy, there should be a high probability to find the presence of a 4_1 helix or gg conformation. The 550 cm^{-1} band can then be used an identification band for such a structure. This band has never been observed in poly(lactic acid) in any of the vibrational spectra obtained. We have studied the as-received pellets, quenched, annealed, or drawn samples carefully. This characteristic band (assigned to be $\delta_1(15)$, $\delta_3(13)$, $\gamma_3(10)$) simply cannot be found. A possible conclusion is that the gg conformation may have much higher energy than the original conformational analysis suggests.

A number of studies have reported that when poly(L-lactic acid) is cocrystallized with its enatiomer, poly(D-lactic acid), a 3_1 helix forms. X-ray experiments on fiber samples of this complex structure have shown there are four possible 3_1 helices.[26] The conformation angles are determined on the basis of a geometrical constraint which requires that three chemical repeats

Table 6. Intensity Parameters Used in Simulation

bond	$C_\alpha-C_\beta$	$C_\alpha-C$	C−O	$O-C_\alpha$	C═O
set A	1.0	1.0	1.0	1.0	1.0
set B	0.6	1.0	1.0	0.5	0.3

angle	$O-C_\alpha-C$	C═O def	$C-O-C_\alpha$	$O-C_\alpha-C_\beta$	$C-C_\alpha-C_\beta$	ipb C═O
set A	0.2	0.02	0.2	0.02	0.4	0.02
set B	0.2	0.1	0.2	0.01	0.01	0.02

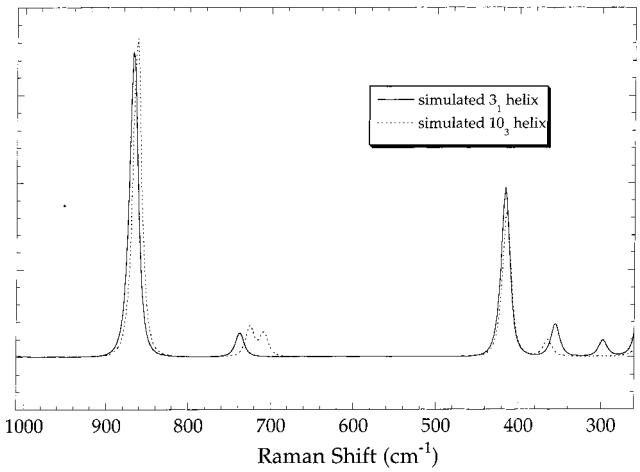

Figure 10. Calculated spectra of 3_1 and 10_3 helix with a different set of intensity parameters.

can finish one turn and that the fiber period is 8.7 Å. Since there are several conformations satisfying this constraint, we were curious whether these structural differences would be present in the samples that we were studying. A conformational energy contour map could not exclude any of the structures. However, the normal-coordinate analysis provides very convincing evidence that only one correct structure exists. Figure 8 shows the simulated Raman spectra of all these possible structures. Models II and III have very strong bands around 800 and 600 cm^{-1}. Model IV has a strong band around 480 cm^{-1}. Not all these bands are observed in any crystalline poly(lactic acid) sample, and none of the simulated spectra of these models are close to the actual crystalline poly(lactic acid) chain conformation. The only choice that fits the data well is model I. On the basis of the normal-coordinate analysis, only one of the four proposed poly(lactic acid) structures is expected.

Finally, on the basis of the success obtained for the various possible 3_1 helices, it is desirable to analyze the features expected for the 10_3 helix. Since 10_3 and 3_1 are so close in conformation (Table 5), there should not be significant differences in Raman or infrared spectra. Figure 9 is the simulated spectra of 10_3 and 3_1. All the bands except the doublet around 700 cm^{-1} region have very similar position and intensity. In the 3_1 helix model, the 736 cm^{-1} band is higher than the 710 cm^{-1} band calculated for a 10_3 model; the 736 cm^{-1} band weakens to become a shoulder while 710 cm^{-1} increases in intensity. Considering the fact that source of the intensity parameters used here has not been precisely determined, an alternative set of parameters was used (Table 6, set B). The results calculated for this set are shown in Figure 10. The doublet components in the 10_3 helix are of equal intensity, but the 300 cm^{-1} band disappears, which is not in agreement with the experimental data obtained. In addition, it is also found that the 736 cm^{-1} band increases in intensity while the 710 cm^{-1} band decreased in 3_1 helix model. This consistent pattern of changing intensity does imply that the relative intensity of the 736 and 710 cm^{-1} bands is a good indicator of the 10_3 and 3_1 helix. For the annealed sample, it seems that 3_1 and 10_3 coexist, considering the relative intensity of this doublet in the data. However, a pure 3_1 helix cannot fit the data perfectly because there are some small peaks such as the 910 or 584 cm^{-1}, which cannot be explained. On the other hand, a pure 10_3 helix also does not fit the data satisfactorily because the 736 cm^{-1} band is too weak compared with the 710 cm^{-1} band according to the above simulation. Our normal-coordinate analysis therefore also suggests that a considerable amount of structural disorder exists, making a clear definition difficult. This conclusion supports the argument made by Brizzolara.[11]

Conclusion

By comparing the calculated spectra with the experimental data, the force constants, structure, and intensity parameters of poly(L-lactic acid) are validated. The four 3_1 helix models predicted in Okihara's experiment can be discriminated and the unrealistic ones excluded. The calculation can further point out that gg conformation of Tonelli's RIS model[13] has much lower probability than expected, or the energy minimum of gg is much higher than that of the gt conformation. Better experiments on well-defined poly(lactic acid) and with solvent that is more versatile may yield a more definitive analysis of chain dimension and associated chain conformations.[7]

References and Notes

(1) Leenslag, J. W.; Pennings, A. J. *Makromol. Chem.* **1987**, *188*, 1809.
(2) Schakenraad, J. M.; Oosterbaan, J. A.; Nieuwenhuis, P.; Molenaar, I.; Olijslager, J.; Potman, W.; Eenink, M. J. D.; Feijen, J. *Biomaterials* **1988**, *9*, 116.
(3) Spenlehauer, G.; Vert, M.; Benoit, J. P.; Boddaert, A. *Biomaterials* **1989**, *10*, 557.
(4) Gilding, D. K.; Reed, A. M. *Polymer* **1979**, *20*, 1459.
(5) Postema, A. R.; Pennings, A. J. *J. Appl. Polym. Sci.* **1989**, *37*, 2351.
(6) Hoogsteen, W.; Postema, A. R.; Pennings, A. J.; Brinke, G. t.; Zugenmaier, P. *Macromolecules* **1990**, *23*, 634.
(7) Grijpma, D. W.; Penning, J. P.; Pennings, A. J. *Colloid Polym. Sci.* **1994**, *272*, 1068.
(8) Huang, J.; Lisowski, M. S.; Runt, J.; Hall, E. S.; Kean, R. T.; Buehler, N.; Lin, J. S. *Macromolecules* **1998**, *31*, 2593.
(9) Bos, R.; Rozema, F. R.; Boering, G.; Nijenhuis, A.; Pennings, A.; Verwey, A. B.; Nijenhuis, P.; Jansen, H. W. B. *Biomaterials* **1991**, *12*, 28.
(10) De Santis, P.; Kovacs, A. J. *Biopolymers* **1968**, *6*, 299.
(11) Brizzolara, D.; Cantow, H.-J.; Diederichs, K.; Keller, E.; Domb, A. J. *Macromolecules* **1996**, *29*, 191.
(12) Brant, D. A.; Tonelli, A. E.; Flory, P. J. *Macromolecules* **1969**, *2*, 228.
(13) Tonelli, A. E.; Flory, P. J. *Macromolecules* **1969**, *2*, 225.
(14) Joziasse, C. A.; Veenstra, H.; Grijpma, D. W.; Pennings, A. J. *Macromol. Chem. Phys.* **1996**, *197*, 2219.
(15) Harrick, N. J. *Internal Reflection Spectroscopy*; John Wiley & Sons: New York, 1967.
(16) Moore, W. H.; Krimm, S. *Biopolymers* **1976**, *15*, 2439.
(17) Snyder, R. G.; Kim, Y. *J. Phys. Chem.* **1991**, *95*, 602.
(18) Snyder, R. G. *J. Chem. Soc., Faraday Trans* **1992**, *88*, 1823.

(19) Tang, J.; Albrecht, A. C. In *Raman Spectroscopy: Theory and Practice*; Szymanski, H. A., Ed.; Plenum Press: New York, 1970; Vol. 2, p 33.
(20) Cates, D. A.; Strauss, H. L.; Snyder, R. G. *J. Phys. Chem.* **1994**, *98*, 4482.
(21) Hallmark, V. M.; Bohan, S. P.; Strauss, H. L.; Snyder, R. G. *Macromolecules* **1991**, *24*, 4025.
(22) Yang, X.; Su, Z.; Wu, D.; Hsu, S. L.; Stidham, H. D. *Macromolecules* **1997**, *30*, 3796.
(23) Hahn, T. D. Ph D. Thesis, University of Massachusetts, 1998.
(24) Tao, H. J.; MacKnight, W. J.; Gagnon, K. D.; Lenz, R. W.; Hsu, S. L. *Macromolecules* **1995**, *28*, 2016.
(25) Hahn, T.; Suen, W.; Kang, S.; Hsu, S. L.; Stidham, H. D.; Siedle, A. R. *Polymer*, in press.
(26) Okihara, T.; Tsuji, M.; Katayama, K.; Kawaguchi, A.; Katayama, K.; Tsuji, H.; Hyon, S.; Ikada, Y. *J. Macromol. Sci., Phys.* **1991**, *B30* (1&2), 119.
(27) Boerio, F. J.; Bahl, S. K. *J. Polym. Sci., Polym. Phys. Ed.* **1976**, *14*, 1029.
(28) Snyder, R. G.; Zerbi, G. *Spectrochim. Acta* **1967**, *23A*, 391.
(29) Bahl, S. K. Ph.D. Dissertation, University of Cincinnati, 1976.
(30) Chang, C.; Wang, Y. K.; Waldman, D. A.; Hsu, S. L. *J. Polym. Sci., Polym. Phys. Ed.* **1984**, *22*, 2185.
(31) McDonald, M. P.; Ward, I. M. *Polymer* **1961**, *2*, 341.
(32) Vasko, P. D.; Koenig, J. L. *Macromolecules* **1970**, *3*, 597.
(33) Bailey, R. T.; Hyde, A. J.; Kim, J. J. *Spectrochim Acta* **1974**, *30A*, 91.
(34) Smith, P. B.; Leugers, A.; Kang, S.; Yang, X.; Hsu, S. L. *J. Appl. Polym. Sci.*, submitted.

MA0016026